DOI: 10.1002/chem.200600960

Rh-Catalyzed Enantioselective Conjugate Addition of Arylboronic Acids with a Dynamic Library of Chiral *tropos* Phosphorus Ligands

Chiara Monti,[a] Cesare Gennari,*[a] and Umberto Piarulli*[b]

Abstract: A library of 19 chiral *tropos* phosphorus ligands, based on a free-to-rotate (*tropos*) biphenol unit and a chiral P-bonded alcohol (11 phosphites, **1**-$P(O)_2O$ to **11**-$P(O)_2O$) or secondary amine (8 phosphoramidites, **12**-$P(O)_2N$ to **19**-$P(O)_2N$), were screened, individually and in combinations of two, in the rhodium-catalyzed asymmetric conjugate addition of arylboronic acids to enones and enoates. High enantioselectivities (up to 99% *ee*) and excellent yields were obtained in the addition to either cyclic or acyclic substrates. The flexible biphenolic P ligands outperformed the analogous rigid binaphtholic P ligands. Variable-temperature ^{31}P NMR studies revealed that the biphenolic ligands are *tropos* even at low temperature. Only below 190 K was a coalescence observed; upon further cooling, two atropisomers were detected. The Rh homocomplexes ($[Rh(L^a)_2]^+$) were also studied: in general, a single doublet (P–Rh coupling) was observed in the case of the biphenolic phosphite ligands, over the temperature range 380–230 K, demonstrating their *tropos* nature in the rhodium complexes even at low temperatures. On the other hand, the phosphoramidites showed different behaviors depending on the structure of the ligand and on the nature of the rhodium source. The spectrum at 230 K of the mixture of $[Rh(acac)(eth)_2]$ (eth = C_2H_4) with phosphite **6**-$P(O)_2O$ and phosphoramidite **19**-$P(O)_2N$ (the most enantioselective ligand combination in the conjugate addition reaction) revealed the presence of four homocomplexes (total approximately 40%: [Rh{**6**-$P(O)_2O$}$_2$], [Rh{(a*R*)-**19**-$P(O)_2N$}$_2$], [Rh{(a*S*)-**19**-$P(O)_2N$}$_2$], [Rh{(a*R*)-**19**-$P(O)_2N$}{(a*S*)-**19**-$P(O)_2N$}]) and one heterocomplex, [Rh{**6**-$P(O)_2O$}{(a*R*)-**19**-$P(O)_2N$}] (approximately 60%) In the heterocomplex, the biphenol-derived phosphite is free to rotate (*tropos*) while the biphenol-derived phosphoramidite shows a temperature-dependent *tropos*/*atropos* behavior (coalescence temperature = 310 K).

Keywords: asymmetric catalysis · atropisomerism · enones · NMR spectroscopy · P ligands · rhodium

Introduction

The asymmetric rhodium-catalyzed conjugate addition of aryl- and vinylboronic acids, originally reported by Miyaura and Hayashi, has become the method of choice for the stereoselective introduction of an aryl or a vinyl group in the β position of a variety of electron-deficient olefins (including enones, nitroolefins, α,β-unsaturated esters, amides, phosphonates, and sulfones).[1] Excellent enantioselectivities were obtained using both bidentate (binap,[2] segphos,[3] chiraphos,[4] P-phos,[5] diphosphonites,[6] bisphosphanes,[7] amidomonophosphanes,[8] chiral dienes,[9] deguPhos,[10] cyrhetrenes,[11]) and more recently monodentate ligands (binaphtholic phosphoramidites), which may contain, besides the stereogenic axis, additional stereogenic elements (stereocenters).[12]

A library of 19 chiral *tropos* phosphorus ligands, based on a flexible (*tropos*)[13] biphenol unit and a chiral P-bonded alcohol (11 phosphites) or secondary amine (8 phosphoramidites), was recently synthesized in our laboratories and used in the rhodium-catalyzed asymmetric hydrogenation of prochiral olefins.[14] These ligands exist as a mixture of two rapidly interconverting diastereomers, L^a and $L^{a'}$, differing in

[a] Dr. C. Monti, Prof. Dr. C. Gennari
Dipartimento di Chimica Organica e Industriale
Centro di Eccellenza C.I.S.I.
Università degli Studi di Milano
Istituto di Scienze e Tecnologie Molecolari (ISTM) del CNR
Via G. Venezian 21, 20133 Milano (Italy)
Fax: (+39) 02-5031-4072
E-mail: cesare.gennari@unimi.it

[b] Prof. Dr. U. Piarulli
Dipartimento di Scienze Chimiche e Ambientali
Università degli Studi dell'Insubria
Via Valleggio 11, 22100 Como (Italy)
Fax: (+39) 031-238-6449
E-mail: umberto.piarulli@uninsubria.it

Supporting information for this article is available on the WWW under http://www.chemeurj.org/ or from the author.

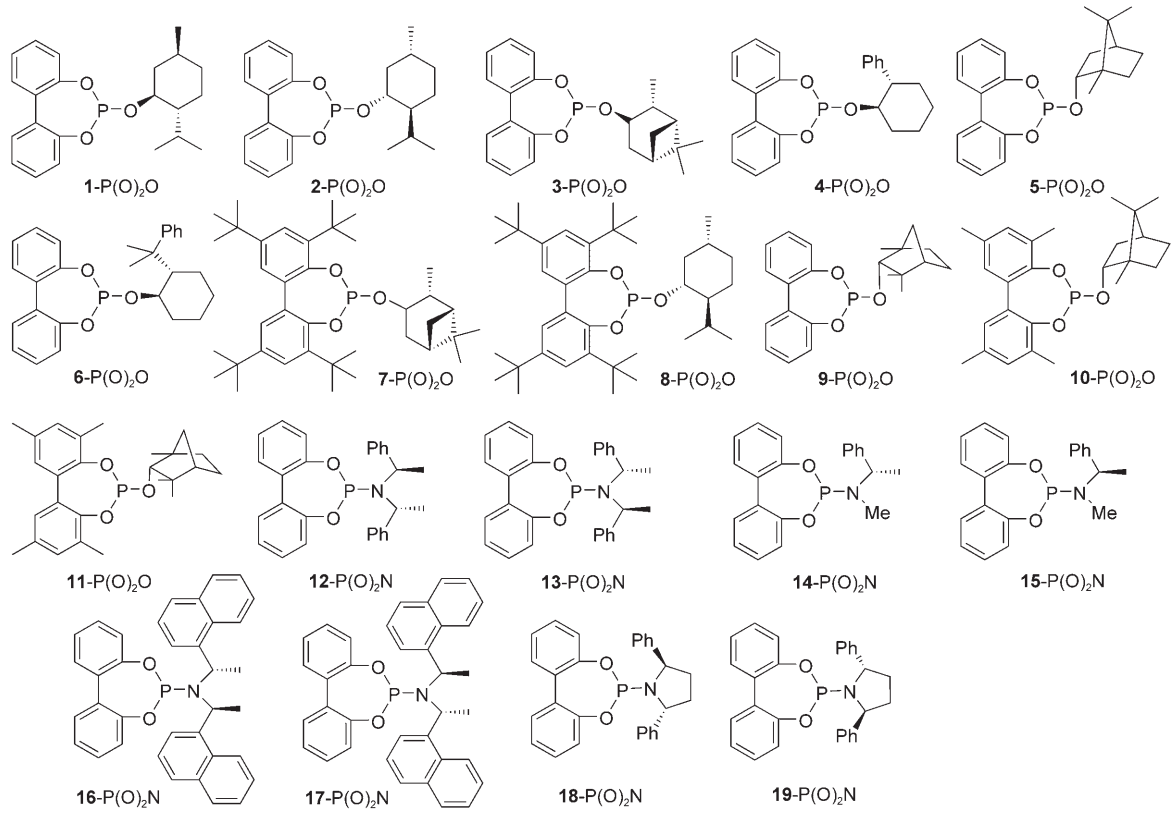

the conformation of the biphenol unit (Scheme 1). Upon complexation with Rh, the ligand (L^a in equilibrium with $L^{a'}$) should give rise to three different species, namely

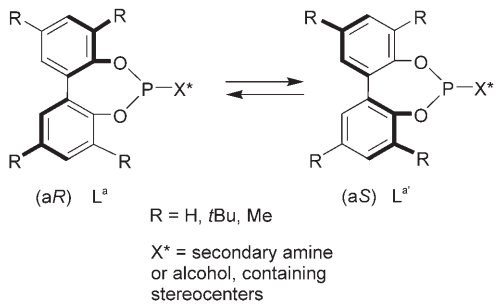

Scheme 1. Chiral phosphorus ligands based on a chiral P-bonded alcohol or secondary amine and a flexible (*tropos*) P-bonded biphenol unit.

$[Rh(L^a)(L^a)]$, $[Rh(L^a)(L^{a'})]$, $[Rh(L^{a'})(L^{a'})]$. These three diastereomeric species, which might be interconverting, are generated in proportions which most probably differ from the statistical value (1:2:1). In this paper we report highly enantioselective rhodium-catalyzed conjugate additions of arylboronic acids to a variety of α,β-unsaturated carbonyl derivatives (cyclic and acyclic enones, α,β-unsaturated lactones and esters) by using a dynamic library of chiral phosphorus ligands, and characterize the *tropos*/*atropos* nature of the ligands in the rhodium complexes by ^{31}P NMR spectroscopy.[15] Following the lead of Reetz and co-workers[16] and Feringa and co-workers,[12b,17] we used a combination of two of these ligands (L^a in equilibrium with $L^{a'}$ and L^b in equilibrium with $L^{b'}$) and generated a dynamic in-situ library,[18] with up to ten different species theoretically present in solution: $[Rh(L^a)(L^a)]$, $[Rh(L^a)(L^{a'})]$, $[Rh(L^{a'})(L^{a'})]$ (homocomplexes with L^a and $L^{a'}$), $[Rh(L^b)(L^b)]$, $[Rh(L^b)(L^{b'})]$, $[Rh(L^{b'})(L^{b'})]$ (homocomplexes with L^b and $L^{b'}$), and $[Rh(L^a)(L^b)]$, $Rh(L^a)(L^{b'})]$, $[Rh(L^{a'})(L^b)]$, $[Rh(L^{a'})(L^{b'})]$ (heterocomplexes). Although, in principle, each species could be present and catalyze the reaction, one of them could predominate over the others, determining the direction and the extent of the enantioselectivity.

Results and Discussion

Asymmetric 1,4-addition of arylboronic acids to enones and enoates: The library of 11 biphenolic phosphites and eight biphenolic phosphoramidites was screened initially in the conjugate addition of phenylboronic acid to 2-cyclohexenone (**20 A**), as a benchmark reaction, by using 1.5 mol% $[\{Rh(eth)_2Cl\}_2]$[19] and a total of 6 mol% of ligands (Rh/L = 1:2) (Scheme 2). The reaction was performed using KOH (1 equiv) as base,[20] in a 10:1 dioxane/water solution at room temperature overnight; a few selected results are presented in Table 1, entries 1–7 (see the Supporting Information for the complete screening results). In general, when the chiral ligands were used individually (homocombinations) the phosphites gave more efficient and enantioselec-

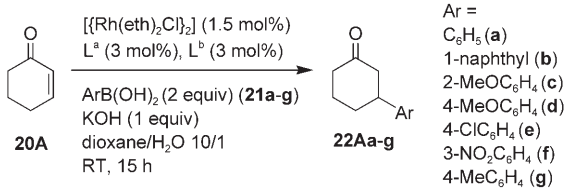

Scheme 2. Rh-catalyzed conjugate addition of arylboronic acids to 2-cyclohexenone (**20A**).

Table 1. Rh-catalyzed conjugate addition of arylboronic acids to 2-cyclohexenone (**20A**): selected results.[a]

Entry	$ArB(OH)_2$	T [°C]	$L^{[a]}$	$L^{[b]}$	Product	Conv. [%][b]	*ee* [%][b]	Abs. conf.
1	**21a**	23	**6**-$P(O)_2O$	**6**-$P(O)_2O$	**22Aa**	100	70	(*R*)-(+)
2	**21a**	23	**19**-$P(O)_2N$	**19**-$P(O)_2N$	**22Aa**	100	36	(*R*)-(+)
3	**21a**	23	**6**-$P(O)_2O$	**19**-$P(O)_2N$	**22Aa**	100	95	(*R*)-(+)
4	**21a**	23	**6**-$P(O)_2O$	**18**-$P(O)_2N$	**22Aa**	100	70	(*S*)-(−)
5	**21a**	23	**9**-$P(O)_2O$	**9**-$P(O)_2O$	**22Aa**	100	28	(*R*)-(+)
6	**21a**	23	**9**-$P(O)_2O$	**19**-$P(O)_2N$	**22Aa**	100	91	(*R*)-(+)
7	**21a**	23	**9**-$P(O)_2O$	**18**-$P(O)_2N$	**22Aa**	100	87	(*S*)-(−)
8	**21b**	23	**6**-$P(O)_2O$	**6**-$P(O)_2O$	**22Ab**	100	42	(+)
9	**21b**	23	**19**-$P(O)_2N$	**19**-$P(O)_2N$	**22Ab**	50	52	(+)
10	**21b**	23	**6**-$P(O)_2O$	**19**-$P(O)_2N$	**22Ab**	95	83	(+)
11	**21b**	23	**9**-$P(O)_2O$	**9**-$P(O)_2O$	**22Ab**	100	23	(+)
12	**21b**	23	**9**-$P(O)_2O$	**18**-$P(O)_2N$	**22Ab**	100	75	(−)
13	**21b**	23	**9**-$P(O)_2O$	**19**-$P(O)_2N$	**22Ab**	100	70	(+)
14	**21c**	23	**6**-$P(O)_2O$	**6**-$P(O)_2O$	**22Ac**	100	41	(*R*)-(+)
15	**21c**	23	**18**-$P(O)_2N$	**18**-$P(O)_2N$	**22Ac**	100	42	(*S*)-(−)
16	**21d**	23	**6**-$P(O)_2O$	**6**-$P(O)_2O$	**22Ad**	100	64	(*R*)-(+)
17	**21d**	23	**19**-$P(O)_2N$	**19**-$P(O)_2N$	**22Ad**	50	6	(*R*)-(+)
18	**21d**	23	**6**-$P(O)_2O$	**19**-$P(O)_2N$	**22Ad**	97	92	(*R*)-(+)
19	**21d**	23	**6**-$P(O)_2O$	**18**-$P(O)_2N$	**22Ad**	95	60	(*S*)-(−)
20	**21e**	23	**6**-$P(O)_2O$	**6**-$P(O)_2O$	**22Ae**	50	58	(+)
21	**21e**	80	**6**-$P(O)_2O$	**6**-$P(O)_2O$	**22Ae**	57	18	(+)
22[c]	**21e**	23	**6**-$P(O)_2O$	**6**-$P(O)_2O$	**22Ae**	100	63	(+)
23[c]	**21e**	23	**19**-$P(O)_2N$	**19**-$P(O)_2N$	**22Ae**	0	nd	–
24[c]	**21e**	23	**6**-$P(O)_2O$	**19**-$P(O)_2N$	**22Ae**	95	85	(+)
25	**21f**	23	**6**-$P(O)_2O$	**6**-$P(O)_2O$	**22Af**	0	nd	–
26	**21f**	80	**6**-$P(O)_2O$	**6**-$P(O)_2O$	**22Af**	0	nd	–
27	**21g**	23	**6**-$P(O)_2O$	**6**-$P(O)_2O$	**22Ag**	100	75	(*R*)-(+)
28	**21g**	23	**19**-$P(O)_2N$	**19**-$P(O)_2N$	**22Ag**	90	41	(*R*)-(+)
29	**21g**	23	**6**-$P(O)_2O$	**19**-$P(O)_2N$	**22Ag**	100	99	(*R*)-(+)

[a] Standard reaction conditions for the library screening: $(L^a + L^b)/[\{Rh(eth)_2Cl\}_2]/ArB(OH)_2/KOH$/2-cyclohexenone = 0.06:0.015:2:1:1. [b] Yields and *ee* values were determined by chiral GC or HPLC (see the Supporting Information). [c] 5 mol% $[\{Rh(eth)_2Cl\}_2]$ and a total of 20 mol% of ligands.

tive catalysts than the phosphoramidites. However, the enantiomeric excesses were only moderate and the best *ee* was 70% with phosphite **6**-$P(O)_2O$ (Table 1, entry 1). Mixtures of a phosphite and a phosphoramidite (heterocombinations) gave reduced yields and *ee* values in comparison with the phosphite alone, in all combinations except those containing either phosphoramidite **18**-$P(O)_2N$ or **19**-$P(O)_2N$. In these heterocombinations, considerably higher *ee* values and quantitative yields were obtained. In particular, (*R*)-3-phenylcyclohexanone (**22Aa**) was obtained in 95% *ee* (100% yield) with phosphoramidite **19**-$P(O)_2N$ and phosphite **6**-$P(O)_2O$ (Table 1, entry 3), and in 91% *ee* (100% yield) with phosphoramidite **19**-$P(O)_2N$ and phosphite **9**-$P(O)_2O$ (Table 1, entry 6). In the latter case, the synergistic effect of the heterocombination with respect to the corresponding homocombinations is worth an additional 55% *ee* (**9**-$P(O)_2O$ 28% *ee*, entry 5; **19**-$P(O)_2N$ 36% *ee*, entry 2). The mismatched combinations gave (*S*)-3-phenylcyclohexanone (**22Aa**) in 70% *ee* (100% yield) with phosphoramidite **18**-$P(O)_2N$ and phosphite **6**-$P(O)_2O$ (Table 1, entry 4), and 87% *ee* (100% yield) with phosphoramidite **18**-$P(O)_2N$ and phosphite **9**-$P(O)_2O$ (Table 1, entry 7), showing that it is the phosphoramidite which determines the absolute configuration of the reaction product. Again, the synergistic effect of the heterocombination is remarkable. The *ee* enhancements with these ligands are notable and generally higher than those obtained using combinations of binaphtholic phosphites or phosphoramidites.[12b,16,17]

The scope of this reaction was then investigated using various arylboronic acids, with 2-cyclohexenone (**20A**) as the substrate (Table 1, entries 8–29; see the Supporting Information for the complete screening results).

In general, the combination of phosphite **6**-$P(O)_2O$ and phosphoramidite **19**-$P(O)_2N$ proved to be the most efficient and enantioselective; as for the arylboronic acids, high yields and excellent *ee* values were obtained with the electron-rich *p*-anisylboronic (**21d**) and *p*-tolylboronic (**21g**) acids. In particular, the **19**-$P(O)_2N$/**6**-$P(O)_2O$ combination gave (3*R*)-3-(4-methoxyphenyl)cyclohexanone (**22Ad**) in 92% *ee* (97% yield; Table 1, entry 18); (3*S*)-3-(4-methoxyphenyl)cyclohexanone (**22Ad**) was obtained in 60% *ee* with the mismatched pair **18**-$P(O)_2N$/**6**-$P(O)_2O$ (Table 1, entry 19). (3*R*)-3-(4-Methylphenyl)cyclohexanone (**22Ag**) was obtained in 99% *ee* (100% yield) using the combination phosphoramidite **19**-$P(O)_2N$/phosphite **6**-$P(O)_2O$ (Table 1, entry 29). Again, the synergistic effect of this heterocombination with respect to the corresponding homocombinations is remarkable (**6**-$P(O)_2O$ 75% *ee*, entry 27; **19**-$P(O)_2N$ 41% *ee*, entry 28). 1-Naphthylboronic (**21b**) and *p*-chlorophenylboronic (**21e**) acids also afforded the expected products with good *ee* values; with the ligand combination **19**-$P(O)_2N$/**6**-$P(O)_2O$, 3-(1-naphthyl)cyclohexanone (**22Ab**) was obtained in 83% *ee* (95% yield, entry 10), and 3-(4-chlorophenyl)cyclohexanone (**22Ae**) was obtained in 85% *ee* (95% yield, entry 24). In contrast, *m*-nitrophenylboronic acid (**21f**) did not react. This observation parallels the lack of reactivity of electron-poor arylboronic acids reported by

Minnaard and co-workers in the Pd-catalyzed conjugate addition reaction.[21] *o*-Tolylboronic acid (**21c**) gave moderate *ee* values and complete conversions when the chiral ligands were used individually (homocombinations, entries 14 and 15), while use of the heterocombinations did not result in any enhancement of the *ee* values. The use of phenylboroxine[22] did not lead to any *ee* enhancement; on the contrary, a slight decrease in the enantioselectivity was observed in all cases: for example, **6**-$P(O)_2O$ gave (*R*)-3-phenylcyclohexanone (**22Aa**) in 60% *ee* (compare entry 1, 70% *ee*), while the combination **19**-$P(O)_2N$/**6**-$P(O)_2O$ gave **22Aa** in 90% *ee* (compare entry 3, 95% *ee*).

The effect of the substrate was then evaluated: the variation of the ring size was investigated by using all the homocombinations and several heterocombinations with 2-cyclopentenone (**20B**) and 2-cycloheptenone (**20C**) (see Table 2 for selected results and the Supporting Information for the complete screening). The best results were again obtained using the heterocombination containing **6**-$P(O)_2O$ and the 2,5-diphenylpyrrolidine phosphoramidite **19**-$P(O)_2N$. This matched combination afforded (*R*)-3-phenyl-cyclopentanone (**22Ba**) in 73% *ee* and 95% yield (Table 2, entry 1) and (*R*)-3-phenyl-cycloheptanone (**22Ca**) in 90% *ee* and 97% yield (Table 2, entry 2).

Acyclic enones were also screened (see Table 2 for selected results and the Supporting Information for the complete screening). In these cases, the homocombination of phosphite **6**-$P(O)_2O$ worked better than the heterocombinations. For example, (4*R*)-4-phenylpentan-2-one (**22Ea**, entry 5) and 4-phenyloctan-2-one (**22Ha**, entry 12) were obtained in reasonable *ee* (75–76%), albeit with incomplete conversions. In contrast, (4*S*)-5-methyl-4-phenylhexan-2-one (**22Fa**, entry 6) and (4*R*)-4-phenylnonan-2-one (**22Ia**, entry 15) were obtained in high *ee* (93% and 92%, respectively) and with good yields (90% and 100%, respectively). The conjugate addition of *p*-anisylboronic acid (**21d**) to 4-phenyl-3-buten-2-one (**20G**) required a higher reaction temperature (80°C) to proceed to completion: **22Gd** was obtained in good *ee* (80%, entry 10).

To study whether the range of substrates could be expanded beyond enones, α,β-unsaturated lactone **20D** was subjected to the same reaction conditions, but only a moderate 50% *ee* was obtained with phosphoramidite **19**-$P(O)_2N$ at 80°C (entry 4). Better results were obtained by addition of *p*-anisylboronic acid (**21d**) to *tert*-butyl 3-phenylpropanoate (**20J**) using phosphite **6**-$P(O)_2O$, with the formation of **22Jd** in 79% *ee* (entry 18).

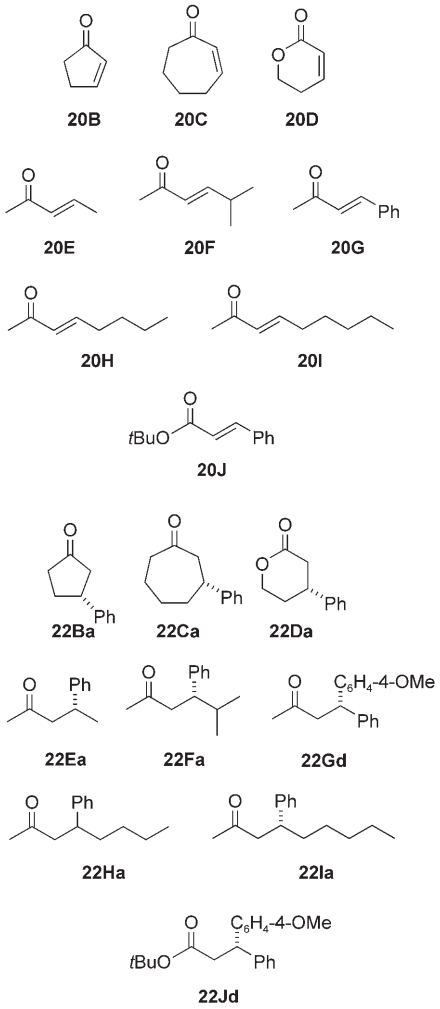

Table 2. Rh-catalyzed conjugate addition of arylboronic acids to substrate **20**: selected results.[a]

Entry	Substrate	$ArB(OH)_2$	*T* [°C]	L[a]	L[b]	Prod.	Conv. [%][b]	*ee* [%][b]	Abs. conf.
1	**20B**	**21a**	23	**6**-$P(O)_2O$	**19**-$P(O)_2N$	**22Ba**	95	73	(*R*)-(+)
2	**20C**	**21a**	23	**6**-$P(O)_2O$	**19**-$P(O)_2N$	**22Ca**	97	90	(*R*)-(+)
3	**20C**	**21a**	23	**9**-$P(O)_2O$	**19**-$P(O)_2N$	**22Ca**	97	90	(*R*)-(+)
4	**20D**	**21a**	80	**19**-$P(O)_2N$	**19**-$P(O)_2N$	**22Da**	80	50	(*R*)-(−)
5[c]	**20E**	**21a**	23	**6**-$P(O)_2O$	**6**-$P(O)_2O$	**22Ea**	75	76	(*R*)-(−)
6	**20F**	**21a**	23	**6**-$P(O)_2O$	**6**-$P(O)_2O$	**22Fa**	90	93	(*S*)-(−)
7	**20F**	**21a**	80	**6**-$P(O)_2O$	**6**-$P(O)_2O$	**22Fa**	90	80	(*S*)-(−)
8	**20F**	**21a**	23	**19**-$P(O)_2N$	**19**-$P(O)_2N$	**22Fa**	5	48	(*S*)-(−)
9	**20F**	**21a**	23	**6**-$P(O)_2O$	**19**-$P(O)_2N$	**22Fa**	85	81	(*S*)-(−)
10	**20G**	**21d**	80	**6**-$P(O)_2O$	**6**-$P(O)_2O$	**22Gd**	100	80	(*S*)-(−)
11	**20G**	**21d**	80	**10**-$P(O)_2O$	**10**-$P(O)_2O$	**22Gd**	85	67	(*S*)-(−)
12	**20H**	**21a**	23	**6**-$P(O)_2O$	**6**-$P(O)_2O$	**22Ha**	72	75	(−)
13	**20H**	**21a**	23	**19**-$P(O)_2N$	**19**-$P(O)_2N$	**22Ha**	40	54	(−)
14	**20H**	**21a**	23	**6**-$P(O)_2O$	**19**-$P(O)_2N$	**22Ha**	50	63	(−)
15	**20I**	**21a**	23	**6**-$P(O)_2O$	**6**-$P(O)_2O$	**22Ia**	100	92	(*R*)-(−)
16	**20I**	**21a**	23	**19**-$P(O)_2N$	**19**-$P(O)_2N$	**22Ia**	5	61	(*R*)-(−)
17	**20I**	**21a**	23	**6**-$P(O)_2O$	**19**-$P(O)_2N$	**22Ia**	97	80	(*R*)-(−)
18	**20J**	**21d**	23	**6**-$P(O)_2O$	**6**-$P(O)_2O$	**22Jd**	95	79	(*S*)-(+)
19	**20J**	**21d**	23	**18**-$P(O)_2N$	**18**-$P(O)_2N$	**22Jd**	5	30	(*S*)-(+)
20	**20J**	**21d**	23	**6**-$P(O)_2O$	**18**-$P(O)_2N$	**22Jd**	100	71	(*S*)-(+)

[a] Standard reaction conditions for the library screening: $(L^a + L^b)/[\{Rh(eth)_2Cl\}_2]]/ArB(OH)_2/KOH$/substrate = 0.06:0.015:2:1:1. [b] Yields and *ee* values were determined by chiral GC or HPLC (see the Supporting Information). [c] 2.5 mol% $[\{Rh(eth)_2Cl\}_2]$ and a total of 10 mol% of ligands.

NMR studies of the ligands and of their Rh complexes: The remarkable increase in enantiomeric excess observed when using combinations of these biphenolic P ligands is rather puzzling. As we expected (see Introduction), the use of a combination of two *tropos* ligands (L^a in equilibrium with $L^{a'}$ and L^b in equilibrium with $L^{b'}$) generates a dynamic in-situ library with up to ten different species theoretically present in solution: $[Rh(L^a)(L^a)]$, $[Rh(L^a)(L^{a'})]$, $[Rh(L^{a'})(L^{a'})]$ (homocomplexes with L^a and $L^{a'}$), $[Rh(L^b)(L^b)]$, $[Rh(L^b)(L^{b'})]$, $[Rh(L^{b'})(L^{b'})]$ (homocomplexes with L^b and $L^{b'}$), and $[Rh(L^a)(L^b)]$, $Rh(L^a)(L^{b'})]$, $[Rh(L^{a'})(L^b)]$, $[Rh(L^{a'})(L^{b'})]$ (heterocomplexes). These complexes are not formed in the statistical ratio and the library composition should reflect their relative stabilities in terms of both electronic (phosphite/phosphoramidite versus phosphite/phosphite versus phosphoramidite/phosphoramidite combinations) and steric effects. To shed light on the "black box" of this catalyst system, we investigated the dynamic behavior of our biphenolic ligands and of their rhodium complexes (precatalysts) by variable-temperature ^{31}P NMR spectroscopy. Several homocomplexes (with the same ligand) and complexes resulting from selected ligand combinations (that is, phosphite **6**-$P(O)_2O$/phosphoramidite **19**-$P(O)_2N$, the most enantioselective ligand combination in the conjugate addition reaction) were investigated.

NMR characterization of the ligands: The ligands were studied by variable-temperature ^{31}P NMR spectroscopy. At room temperature a single resonance was observed, which corresponds to a free-to-rotate (*tropos*) ligand. The multiplicity did not change over the temperature range 380–210 K. However, by lowering the temperature below 210 K, the singlet corresponding to the *tropos* ligand broadened and eventually split into two signals with coalescence temperatures in the range 200–180 K. In the case of phosphite **4**-$P(O)_2O$, for example, the coalescence temperature is around 190 K (Figure 1). Further cooling (to 183 K) resulted in the generation of two resolved signals approximately in a 2:1 ratio, originating from the two atropisomers. In the case of phosphite **6**-$P(O)_2O$, the coalescence temperature is around 197 K and two broad resonances were observed at 183 K, in a relative ratio of 6.7:1. In these two cases, the free-energy barrier $\Delta G^{\neq}$ to biphenol rotation was calculated[23] to be 8.5 kcal mol^{-1} (see the Supporting Information).[24]

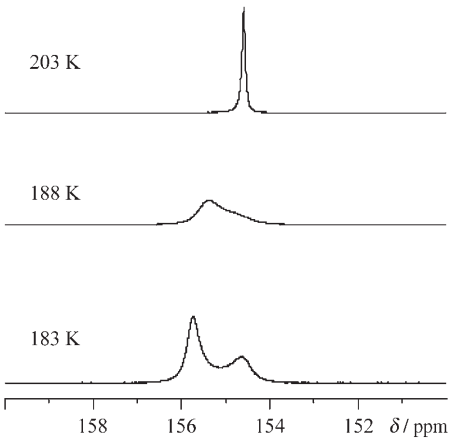

Figure 1. Variable-temperature ^{31}P NMR spectra of ligand **4**-$P(O)_2O$.

NMR studies of the Rh complexes—ligand homocombinations: The *tropos*/*atropos* nature[13] of the ligands in the rhodium complexes was then studied in detail. The metal complexes containing biphenolic *tropos* ligands (phosphites or phosphoramidites) were defined as "induced atropisomeric" by Alexakis[25] and "fluxionally atropisomeric" by Reetz.[16f] However, no evidence was ever presented regarding their *tropos* or *atropos* nature.[26] The variable-temperature ^{31}P NMR spectroscopy of the rhodium complexes originating from several ligand homocombinations ($2L^a$) and different rhodium sources was therefore studied over the temperature range 380–230 K. The temperature could not be lowered below 230 K because of signal broadening caused by the increased viscosity of the sample and precipitation of the rhodium complexes.

In general, a doublet was observed for the rhodium complexes of the phosphites over the temperature range 380–230 K, using $[Rh(acac)(eth)_2]$ as the metal source; this demonstrates the *tropos* nature of the biphenolic phosphites in the $[Rh(acac)(L)_2]$ complexes even at low temperatures.[27] For example, a doublet ($J_{P,Rh}=296$ Hz, $[D_8]$toluene) was observed for the rhodium complex of phosphite **6**-$P(O)_2O$ over the temperature range 380–230 K (Figure 2; see the Supporting Information for the ^{31}P NMR spectra).[28]

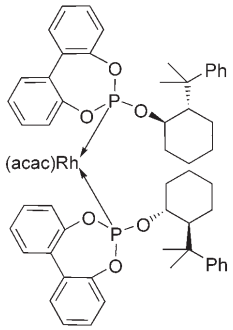

Figure 2. The *tropos* nature of the biphenolic phosphite **6**-$P(O)_2O$ in the Rh complex.

Surprisingly, the rhodium complexes of the phosphoramidites showed a quite diversified and sometimes abnormal behavior, depending on the structure of the phosphoramidite ligand and on the nature of the rhodium source, as discussed below.

*$[Rh(acac)(eth)_2]$ and phosphoramidite **13**-$P(O)_2N$ (or **12**-$P(O)_2N$)*: The ^{31}P NMR spectra of the complex derived from $[Rh(acac)(eth)_2]$ and phosphoramidite **13**-$P(O)_2N$ (or **12**-$P(O)_2N$) at room temperature showed two doublets in addition to the doublet originating from complex [LRh(acac)],

which was visible at ligand/Rh ratios $\leq$ 2:1. The ratio of the two doublets varied, depending on the solvent used, between 1.5:1 ([D_2]dichloromethane) and 3:1 ([D_8]toluene), but was constant with the temperature over the range 380–210 K, and was independent of the ligand/rhodium ratio (Figure 3).

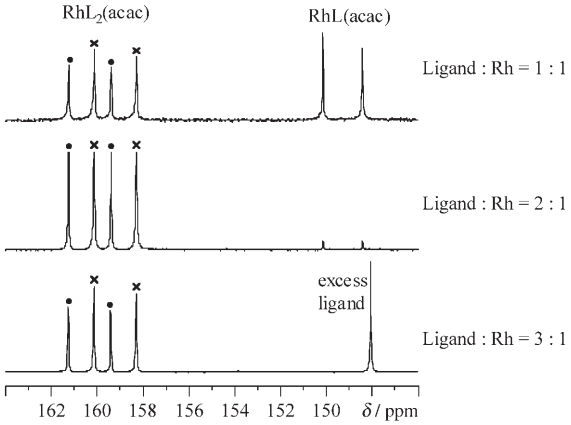

Figure 3. ^{31}P NMR spectra ([D_2]dichloromethane) at 298 K of the rhodium complexes of ligand **13**-P(O)$_2$N, using [Rh(acac)(eth)$_2$] (two doublets: ● and ×), varying the ligand/rhodium ratio.

The ^{31}P NMR spectra of the complexes derived from [Rh(acac)(eth)$_2$] and phosphoramidites **14**-P(O)$_2$N (or **15**-P(O)$_2$N) and **16** P(O)$_2$N (or **17**-P(O)$_2$N) showed, in each case, a doublet at room temperature, which was not broadened by cooling to 230 K. However, when the temperature was lowered an additional doublet was detected, showing that in these cases also an additional species is present and that the two doublets are accidentally isochronous at room temperature (see the Supporting Information).

A control experiment carried out using [Rh(acac)(eth)$_2$] and the (*S*)-binaphthol-derived phosphoramidite **23**-P(O)$_2$N (Figure 4) (an analogue of phosphoramidite **13**-P(O)$_2$N) showed a single sharp doublet over the same temperature range.

However, we tend to exclude the possibility that the two doublets observed in the spectra of the biphenolic phosphoramidite Rh complexes are caused by the biphenol atropisomerism: in fact three diastereomeric complexes (a*R*,a*R*; a*S*,a*S*; a*R*,a*S*) would be expected in this case. Moreover, in the atropisomeric (a*R*,a*S*) complex the two phosphorus atoms are diastereotopic and would couple with rhodium and with each other, giving origin to two doublets of doublets (dd) and *not* to a single doublet (see the relevant discussion below, next section).

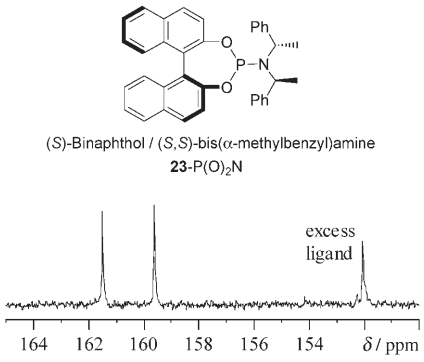

Figure 4. ^{31}P NMR spectrum ([D_2]dichloromethane) at 298 K of the rhodium complex of binaphtholic ligand **23**-P(O)$_2$N, using [Rh(acac)(eth)$_2$].

Alternatively, two different complexes, namely [Rh(acac)(L)$_2$] and [Rh(L)$_4$]$^+$, could account for the observed two doublets. However, this explanation does not fit with: 1) the absence of dependence of the two signals on the Rh/L ratio, and 2) the magnitude of the Rh–L coupling constant $J_{P,Rh}$.[29] Furthermore, all attempts to identify an [Rh(L)$_4$]$^+$ complex by ESI-HRMS were unsuccessful (whereas [Rh(acac)(L)$_2$] was always clearly visible). We tentatively explain the two doublets as the signals of the expected square-planar monomeric complex [Rh(acac)(L)$_2$] (with *tropos* ligands) and of a dinuclear complex containing bridging ligands.[30,31]

*[Rh(acac)(eth)$_2$] and either phosphoramidite **19**-P(O)$_2$N or **18**-P(O)$_2$N*: The ^{31}P NMR spectra of the rhodium complex derived from [Rh(acac)(eth)$_2$]] and either phosphoramidite **19**-P(O)$_2$N or **18**-P(O)$_2$N showed a typical coalescence behavior. In fact, the spectrum at 380 K (Figure 5, top trace)

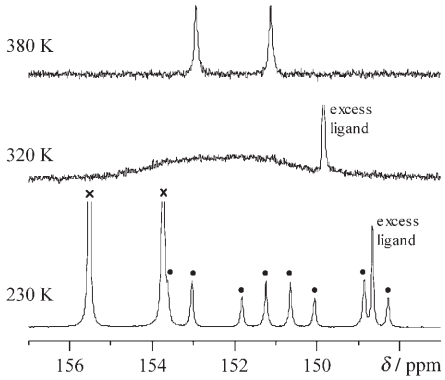

Figure 5. Variable-temperature ^{31}P NMR spectra ([D_8]toluene) of the rhodium complexes of ligand **19**-P(O)$_2$N, with [Rh(acac)(eth)$_2$] as the rhodium source. At 230 K, [Rh{(a*S*)-**19**-P(O)$_2$N}{(a*R*)-**19**-P(O)$_2$N}] gives two dds (●), whereas the doublets of [Rh{(a*R*)-**19**-P(O)$_2$N}$_2$] and [Rh{(a*S*)-**19**-P(O)$_2$N}$_2$] are isochronous (×).

consists of a doublet (δ = 152.0 ppm, $J_{P,Rh}$ = 294 Hz), which, upon cooling, broadens and coalesces at 320 K (Figure 5, middle trace). Further cooling results in the generation of multiple species which at 230 K give origin to a sharp doublet (δ = 154.6 ppm, $J_{P,Rh}$ = 290 Hz) and two doublets of doublets (δ = 152.4 ppm, $J_{P,Rh}$ = 291.8 Hz, $J_{P,P}$ = 95 Hz; δ = 149.5 ppm, $J_{P,Rh}$ = 289.5 Hz, $J_{P,P}$ = 95 Hz) (Figure 5, bottom trace). This can be interpreted as the formation of three diastereomers (a*R*,a*R*; a*S*,a*S*; a*R*,a*S*) differing in the configuration at the two atropisomeric biphenols (which can be a*R* or a*S*), while the configuration of the two amine stereocenters

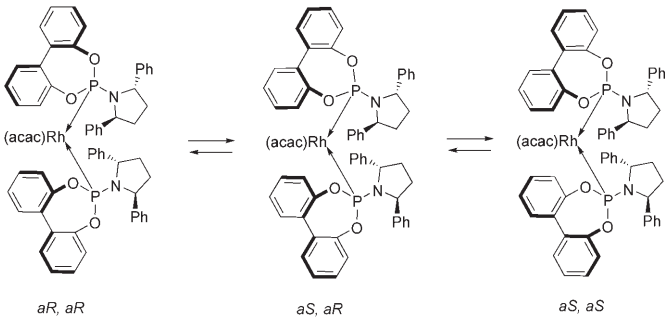

Scheme 3. The *atropos* nature of the biphenolic phosphoramidite **19**-$P(O)_2N$ in the Rh complex, at low temperature (230 K).

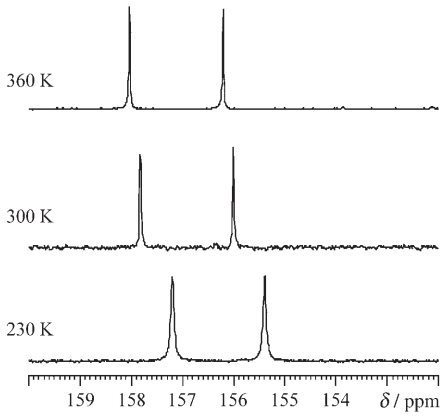

Figure 6. Variable-temperature ^{31}P NMR spectra ([D_8]toluene) of the rhodium complex of ligand **25**-$P(O)_2N$, with [Rh(acac)(eth)$_2$] as the rhodium source.

is clearly fixed (2*S*,5*S*) (Scheme 3). The two diastereomers a*R*,a*R* and a*S*,a*S*, where the two phosphorus atoms are homotopic, give rise to two doublets (P–Rh coupling), which are accidentally isochronous.

In contrast, the a*R*,a*S* diastereomer in which the two phosphorus atoms are diastereotopic and couple with rhodium and with the other phosphorus, gives origin to two doublets of doublets (dd). The free-energy barrier $\Delta G^{\neq}$ to biphenol rotation in [D_8]toluene, calculated from the dd signals,[23], is 14.4 ± 0.2 kcal mol^{-1} (coalescence temperature $T_C = 320$ K), while in [D_2]dichloromethane $\Delta G^{\neq}$ is 13.0 ± 0.2 kcal mol^{-1} ($T_C = 290$ K).

As a further proof that the coalescence behavior of the rhodium complex of phosphoramidite **19**-$P(O)_2N$ (or **18**-$P(O)_2N$) is due to the hindered rotation about the biphenolic axis, and is not ascribable to the conformational properties of the 2,5-diphenylpyrrolidine moiety, we synthesized the binaphtholic phosphoramidites **24**-$P(O)_2N$ and **25**-$P(O)_2N$ which are the (*R*)-binaphthol (or (*S*)-binaphthol)

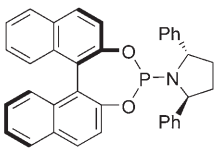

(*R*)-Binaphthol / (*S*,*S*)-2,5-diphenylpyrrolidine
24-$P(O)_2N$

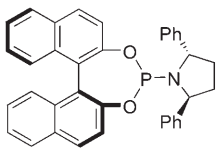

(*S*)-Binaphthol / (*S*,*S*)-2,5-diphenylpyrrolidine
25-$P(O)_2N$

analogues of phosphoramidite **19**-$P(O)_2N$. The rhodium complex of phosphoramidite **25**-$P(O)_2N$ (or **24**-$P(O)_2N$) gave a sharp doublet over the temperature range 380–230 K (Figure 6).

*[Rh(nbd)$_2$][BF$_4$] (nbd = norbornadiene) or [Rh(cod)$_2$][BF$_4$] (cod = 1,4-cyclooctadiene) and phosphoramidites **12**-$P(O)_2N$ (or **13**-$P(O)_2N$), **14**-$P(O)_2N$ (or **15**-$P(O)_2N$), **16** $P(O)_2N$ (or **17**-$P(O)_2N$)*: The ^{31}P NMR spectra of the complexes derived from [Rh(nbd)$_2$][BF$_4$] (nbd = norbornadiene) or [Rh(cod)$_2$][BF$_4$] (cod = 1,4-cyclooctadiene) as rhodium sources and phosphoramidites **12**-$P(O)_2N$ (or **13**-$P(O)_2N$), **14**-$P(O)_2N$ (or **15**-$P(O)_2N$), **16** $P(O)_2N$ (or **17**-$P(O)_2N$) showed a single sharp doublet ($J_{P,Rh} = 290$–300 Hz) over the temperature range 380–230 K. This demonstrates the *tropos* nature of these biphenolic phosphoramidites in the [Rh(L)$_2$(nbd)][BF$_4$] or [Rh(L)$_2$(cod)][BF$_4$] complexes, even at low temperatures.

*[Rh(cod)$_2$][BF$_4$] with phosphoramidites **18**-$P(O)_2N$ (or **19**-$P(O)_2N$)*: With phosphoramidites **18**-$P(O)_2N$ (or **19**-$P(O)_2N$) and [Rh(cod)$_2$][BF$_4$] as the rhodium source, the ^{31}P NMR spectra of the complex showed broad signals and multiple species, even at room temperature. This can be attributed both to the *tropos*/*atropos* behavior of these phosphoramidites (see the relevant discussion above), and to the presence of the cod ligand, which can occasionally display a fluxional behavior.[32] For example, when [Rh(cod)$_2$][BF$_4$] and the atropisomeric binaphtholic phosphoramidite (*S*)-monophos (**26**-$P(O)_2N$) are used, the complex shows a doublet at 325 K ($\delta = 137.7$ ppm, $J_{P,Rh} = 247.8$ Hz), a broad signal typical of a coalescence behavior at 300 K, and one doublet ($\delta = 138.6$ ppm, $J_{P,Rh} = 234.1$ Hz; both cod double bonds are Rh-bonded and the monophos P atoms are homotopic) and two doublets of doublets ($\delta = 134.6$ ppm, $J_{P,Rh} = 240.4$ Hz, $J_{P,P} = 36.8$ Hz; $\delta = 141.0$ ppm, $J_{P,Rh} = 240.7$ Hz, $J_{P,P} = 38.0$ Hz; only one cod double bond is bound to Rh and the monophos P atoms are diastereotopic) at 230 K (total: ten lines). Repeating the same experiment with monophos and [Rh(nbd)$_2$][BF$_4$] as the rhodium source (in which norbornadiene is locked in a boat conformation; Figure 7), a clean

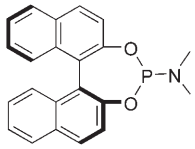

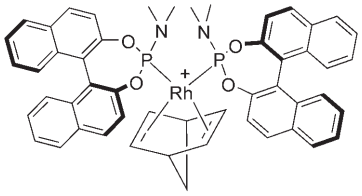

Figure 7. [Rh(nbd)(monophos)$_2$][BF$_4$] complex: P atoms are homotopic (^{31}P NMR spectrum: one doublet with P–Rh coupling).

doublet was observed over the temperature range 380–230 K. Interested researchers should, therefore, be very cautious about the use of [Rh(cod)$_2$][BF$_4$] as the rhodium source for NMR studies.

NMR studies of the Rh complexes—ligand heterocombinations: The rhodium complexes resulting from the combination of phosphite **6**-P(O)$_2$O and phosphoramidite **19**-P(O)$_2$N (the most enantioselective ligand combination in the conjugate addition reaction), with [Rh(acac)(eth)$_2$] as the rhodium source, were studied by variable-temperature ^{31}P NMR spectroscopy. The spectra (Figure 8) account for the presence of all the signals described above due to the [Rh(L^a)(L^a)] and [Rh(L^b)(L^b)] homocomplexes (approximately 40%) and of the new signals for the [Rh(L^a)(L^b)] heterocomplex (approximately 60%). At 375 K (Figure 8, top trace), the heterocomplex [Rh{**6**-P(O)$_2$O}{**19**-P(O)$_2$N}] gives origin to two doublets of doublets (each phosphorus couples with rhodium and with the other phosphorus), which can be interpreted as both a *tropos* phosphite and a *tropos* phosphoramidite. At the coalescence temperature (T_C = 310 K, Figure 8, middle trace), only the signals belonging to the *tropos* phosphite are resolved, that is, a doublet of doublets for the phosphite phosphorus of [Rh{**6**-P(O)$_2$O}{**19**-P(O)$_2$N}] (δ = 157.7 ppm, dd, $J_{P,Rh}$ = 303.2 Hz, $J_{P,P}$ = 100.3 Hz), while the signals of the phosphoramidite are broadened by the coalescence. On cooling to 230 K, the signals of the phosphoramidite are resolved and two doublets of doublets of the [Rh{**6**-P(O)$_2$O}{**19**-P(O)$_2$N}] heterocomplex (δ = 159.5 ppm, dd, $J_{P,Rh}$ = 301.5 Hz, $J_{P,P}$ = 102.0 Hz; δ = 153.2 ppm, dd, $J_{P,Rh}$ = 281.9 Hz, $J_{P,P}$ = 101.9 Hz) can be observed clearly (Figure 8, bottom trace; see the Supporting Information for more details). This can be interpreted by the formation of one of the two possible diastereomers differing in the configuration at the phosphoramidite atropisomeric biphenol (which can be a*R* or a*S*), while the phosphite biphenol remains free to rotate (*tropos*). The free-energy barrier $\Delta G^{\neq}$ to biphenol rotation in the [Rh(L^a)(L^b)] heterocomplex in [D$_8$]toluene was calculated to be 14.5 ± 0.2 kcal mol^{-1} (coalescence temperature T_C = 310 K).[23]

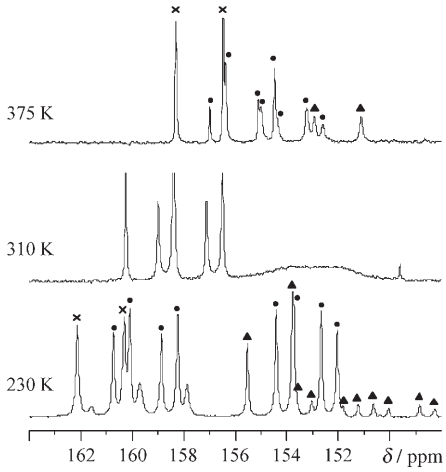

Figure 8. Variable-temperature ^{31}P NMR spectra ([D$_8$]toluene) of the rhodium complexes resulting from the combination of ligands **6**-P(O)$_2$O and **19**-P(O)$_2$N, with [Rh(acac)(eth)$_2$] as the rhodium source. At 375 K, [Rh{**6**–P(O)$_2$O}$_2$] gives a doublet (×), [Rh{**19**-P(O)$_2$N}$_2$] gives a doublet (▲), and [Rh{**6**-P(O)$_2$O}{**19**-P(O)$_2$N}] gives two dds (●); at 230 K, [Rh{**19**-P(O)$_2$N}$_2$] gives two dds (▲) and a doublet (▲), [Rh{**6**-P(O)$_2$O}$_2$] gives a doublet (×), and [Rh{(a*R*)-**19**-P(O)$_2$N}{**6**-P(O)$_2$O}] gives two dds (●).

In summary, of the ten possible different precatalysts, we detected the presence of five species: four homocomplexes (total: approximately 40%) [Rh{**6**-P(O)$_2$O}$_2$], [Rh{(a*R*)-**19**-P(O)$_2$N}$_2$], [Rh{(a*S*)-**19**-P(O)$_2$N}$_2$], [Rh{(a*R*)-**19**-P(O)$_2$N}{a*S*)-**19**-P(O)$_2$N}], and one heterocomplex (approximately 60%) [Rh{**6**-P(O)$_2$O}{(a*R*)-**19**-P(O)$_2$N}] or [Rh{**6**-P(O)$_2$O}{(a*S*)-**19**-P(O)$_2$N}]) (Scheme 4).

To guess reasonably which diastereomer, [Rh{**6**-P(O)$_2$O}{(a*R*)-**19**-P(O)$_2$N}] or [Rh{**6**-P(O)$_2$O}{(a*S*)-**19**-P(O)$_2$N}], is the heterocomplex observed at low temperature, we prepared the (*R*)- and the (*S*)-binaphthol analogues of phosphoramidite **19**-P(O)$_2$N (**24**-P(O)$_2$N and **25**-P(O)$_2$N, respectively) and tested these structurally related ligands separately and in combination with phosphite **6**-P(O)$_2$O in the conjugate addition reaction. Surprisingly, the combinations of **6**-P(O)$_2$O with either the (*S*)-binaphthol analogue **25**-P(O)$_2$N (50% yield, 46% *ee*, (*R*)) or the (*R*)-binaphthol analogue **24**-P(O)$_2$N (70% yield, 72% *ee*, (*R*)) were both considerably less effective than the original biphenol-based combination (Table 3; compare entries 5–7). On the basis of these experiments, the heterocomplex observed at low temperature is presumably the [Rh{**6**-P(O)$_2$O}{(a*R*)-**19**-P(O)$_2$N}] diastereomer.

In the case of the combination of phosphite **6**-P(O)$_2$O and phosphoramidite **18**-P(O)$_2$N (the mismatched ligand combination in the conjugate addition reaction), with [Rh(acac)-(eth)$_2$] as the rhodium source, the low-temperature (230 K) ^{31}P NMR spectrum consisted of the signals attributed to the corresponding homocombinations ([Rh(L^a)(L^a)] and [Rh(L^b)(L^b)]) plus two sets of two doublets of doublets (total: 16 lines) attributed to the heterocomplex [Rh(L^a)(L^b)]. These are caused by the presence of two diastereomers, [Rh{**6**-P(O)$_2$O}{(a*R*)-**18**-P(O)$_2$N}] and [Rh{**6**-P(O)$_2$O}{(a*S*)-**18**-P(O)$_2$N}] (ratio 85:15 or 15:85), differing in the configuration at the phosphoramidite atropisomeric biphenol (Figure 9; see the Supporting Information for more details). In this case, of the ten possible different precatalysts, we detected the presence of six species: four homocomplexes (total: approximately 28%) [Rh{**6**-P(O)$_2$O}$_2$], [Rh{(a*R*)-**18**-P(O)$_2$N}$_2$], [Rh{(a*S*)-**18**-P(O)$_2$N}$_2$], [Rh{(a*R*)-

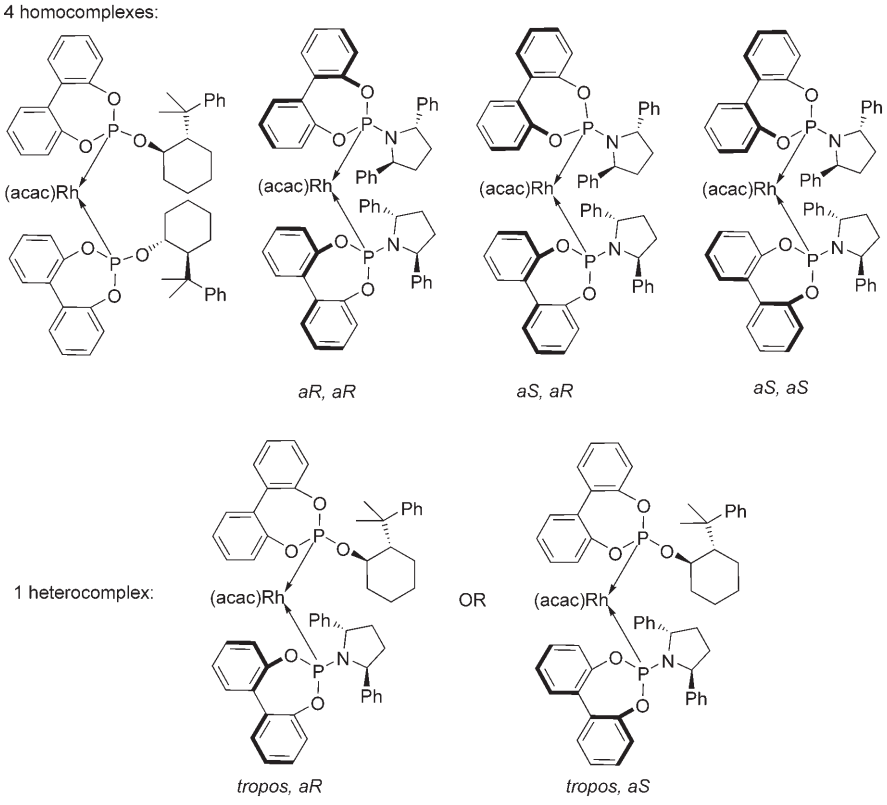

Scheme 4. The rhodium complexes ([Rh(acac)(eth)$_2$] as the rhodium source) that originate from the combination of phosphite **6**-P(O)$_2$O and phosphoramidite **19**-P(O)$_2$N, at low temperature (230 K).

Table 3. Rh-catalyzed conjugate addition of phenylboronic acids to 2-cyclohexenone.[a]

Entry	L[a]	L[b]	Conv. [%][b]	*ee* [%][b]	Abs. conf.
1	**6**-P(O)$_2$O	**6**-P(O)$_2$O	100	70	(*R*)
2	**19**-P(O)$_2$N	**19**-P(O)$_2$N	100	36	(*R*)
3	**24**-P(O)$_2$N	**24**-P(O)$_2$N	40	40	(*R*)
4	**25**-P(O)$_2$N	**25**-P(O)$_2$N	50	28	(*R*)
5	**6**-P(O)$_2$O	**19**-P(O)$_2$N	100	95	(*R*)
6	**6**-P(O)$_2$O	**24**-P(O)$_2$N	70	72	(*R*)
7	**6**-P(O)$_2$O	**25**-P(O)$_2$N	50	46	(*R*)

[a] Standard reaction conditions for the library screening: (L^a + L^b)/[{Rh(eth)$_2$Cl}$_2$]/PhB(OH)$_2$/KOH/2-cyclohexenone = 0.06:0.015:2:1:1.
[b] Yields and *ee* values were determined by chiral GC (see the Supporting Information).

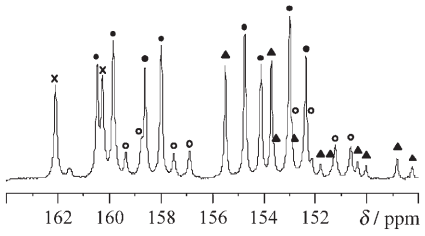

Figure 9. ^{31}P NMR spectra ([D$_8$]toluene) at 230 K of the rhodium complexes resulting from the mismatched combination of ligands **6**-P(O)$_2$O and **18**-P(O)$_2$N, using [Rh(acac)(eth)$_2$] as the rhodium source. At 230 K, [Rh{**18**-P(O)$_2$N}$_2$] gives two dds (▲) and a doublet (▲), [Rh{**6**-P(O)$_2$O}$_2$] gives a doublet (×), [Rh{(a*R*)-**18**-P(O)$_2$N}{**6**-P(O)$_2$O}] gives two dds (● or ○), and [Rh{[(a*S*)-**18**-P(O)$_2$N}{**6**-P(O)$_2$O}] gives two dds (● or ○).

18-P(O)$_2$N}{(a*S*)-**18**-P(O)$_2$N}], and two heterocomplexes (approximately 72%) [Rh{**6**-P(O)$_2$O}{(a*R*)-**18**-P(O)$_2$N}] and [Rh{**6**-P(O)$_2$O}{(a*S*)-**18**-P(O)$_2$N}] in a relative ratio 85:15 or 15:85 (Scheme 5). The free-energy barrier to the biphenol rotation in the [Rh(L^a)(L^b)] heterocomplex had the same value as for the matched pair: in [D$_8$]toluene $\Delta G^{\neq} = 14.5 \pm 0.2$ kcal mol^{-1} (coalescence temperature T_C = 310 K).

Conclusions

A library of 19 chiral *tropos* phosphorus ligands, based on a free-to-rotate (*tropos*) biphenol unit and a chiral P-bonded alcohol (11 phosphites, **1**-P(O)$_2$O to **11**-P(O)$_2$O) or secondary amine (eight phosphoramidites, **12**-P(O)$_2$N to **19**-P(O)$_2$N), were screened, individually and as combinations of two, in the rhodium-catalyzed asymmetric conjugate addition of arylboronic acids to enones and enoates. The scope of the reaction (different boronic acids and substrates) was investigated, and high enantioselectivities as well as excellent yields were observed in the addition to cyclic and acyclic α,β-unsaturated carbonyl derivatives. In particular, in the case of cyclic enones the best results were obtained using the ligand combination phosphite **6**-P(O)$_2$O/phosphoramidite **19**-P(O)$_2$N (99% *ee* in the conjugate addition of *p*-tolylboronic acid to cyclohexenone), while for acyclic substrates, phosphite **6**-P(O)$_2$O alone was preferred. Variable-temperature ^{31}P NMR studies revealed that the biphenolic phosphorus ligands are *tropos* even at low temperature. Only below 190 K was a coalescence observed; upon further cooling, two atropisomers were detected. The composition and the dynamic behavior of the rhodium complexes containing either the single ligands (homocomplexes, [Rh(L^a)(L^a)]$^+$) or the combination of a phosphite and a phosphoramidite (heterocomplexes, [Rh(L^a)(L^b)]$^+$) were studied by variable-temperature ^{31}P NMR spectroscopy. In general, a doublet (P–Rh coupling) was observed in the case of phosphite ligands over the temperature range 380–230 K and using [Rh(acac)(eth)$_2$] as the metal source; this demonstrates the *tropos* nature of the biphenolic phosphites in the [L$_2$Rh(acac)] complexes even at low temperatures. The phosphoramidites showed different behaviors depending on the structure of the ligand and on the nature of the rhodium sources. In particular, two different doublets were detected by ^{31}P NMR in

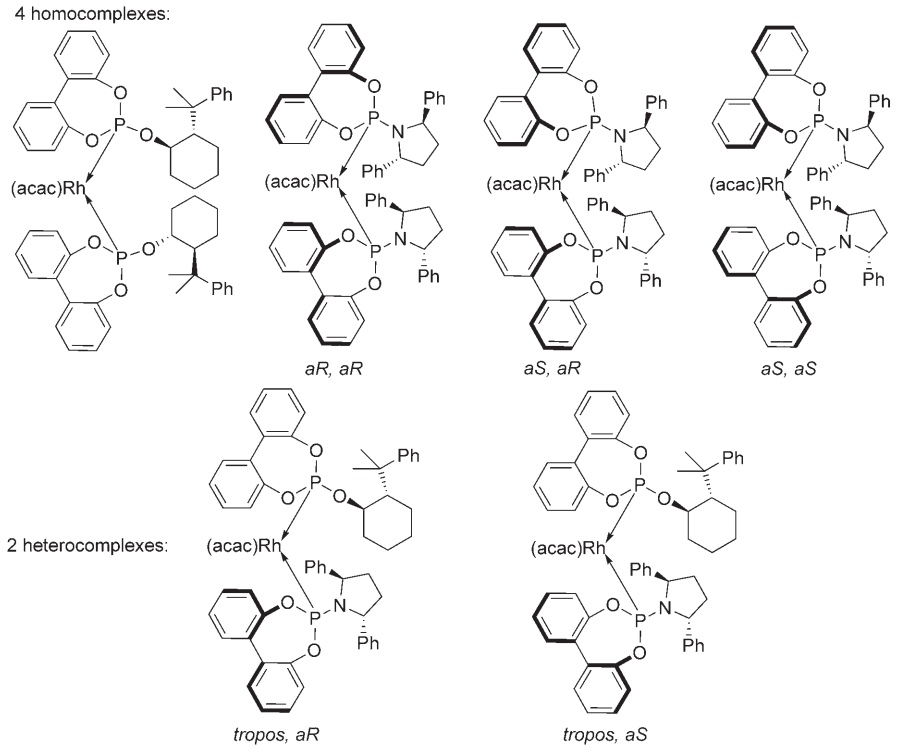

Scheme 5. The rhodium complexes ([Rh(acac)(eth)$_2$] as the rhodium source) that originate from the mismatched combination of phosphite **6**-P(O)$_2$O and phosphoramidite **18**-P(O)$_2$N, at low temperature (230 K).

the homocomplexes of phosphoramidites **12**-P(O)$_2$N to **17**-P(O)$_2$N and [Rh(acac)(eth)$_2$], which are possibly due to the presence of two species, a square-planar monomeric complex and a dinuclear complex containing bridging ligands. Homocomplexes of the same phosphoramidites **12**-P(O)$_2$N to **17**-P(O)$_2$N and either [Rh(cod)$_2$][BF$_4$] or [Rh(nbd)$_2$][BF$_4$] showed the presence of only one doublet and no coalescence over the 380–230 K temperature range. Homocomplexes of phosphoramidites **18**-P(O)$_2$N and **19**-P(O)$_2$N with [Rh(acac)(eth)$_2$] showed a single doublet at 375 K, a coalescence at 320 K, and the generation of a sharp doublet and two doublets of doublets at 230 K. This can be interpreted as the formation of three diastereomers (a*R*,a*R*; a*S*,a*S*; a*R*,a*S*) differing in the configuration at the two atropisomeric biphenols. In the most enantioselective ligand combination in the conjugate addition reaction (that of phosphite **6**-P(O)$_2$O and phosphoramidite **19**-P(O)$_2$N), with [Rh(acac)(eth)$_2$] as the rhodium source, the biphenol-derived phosphite is free to rotate (*tropos*) while the biphenol-derived phosphoramidite shows a temperature-dependent *tropos*/*atropos* behavior (coalescence temperature = 310 K). The spectrum at low temperature accounts for the presence of the signals due to four homocomplexes (total: approximately 40%) [Rh[**6**-P(O)$_2$O]$_2$], [Rh{(a*R*)-**19**-P(O)$_2$N}$_2$], [Rh{(a*S*)-**19**-P(O)$_2$N}$_2$], [Rh{(a*R*)-**19**-P(O)$_2$N}{(a*S*)-**19**-P(O)$_2$N}], and one heterocomplex [Rh{**6**-P(O)$_2$O}{(a*R*)-**19**-P(O)$_2$N}] (approximately 60%). In the case of the combination of phosphite **6**-P(O)$_2$O and phosphoramidite **18**-P(O)$_2$N (the mismatched ligand combination in the conjugate addition reaction) with [Rh(acac)(eth)$_2$] as the rhodium source, the presence of six of the ten possible different precatalysts was detected at low temperature: the four homocomplexes (total: approximately 28%), and two heterocomplexes (approximately 72%) [Rh[**6**-P(O)$_2$O}{(a*R*)-**18**-P(O)$_2$N}] and [Rh{**6**-P(O)$_2$O}{(a*S*)-**18**-P(O)$_2$N}] in a relative ratio 85:15 or 15:85.

From the experimental results of the Rh-catalyzed conjugate addition reactions and from the ^{31}P NMR studies of the Rh precatalysts, it is evident that: 1) the synergistic effect (resulting in notable *ee* enhancements) of the phosphite **6**-P(O)$_2$O/phosphoramidite **19**-P(O)$_2$N ligand heterocombination is remarkable; and 2) the flexible biphenolic P ligands outperform the analogous rigid binaphtholic P ligands (Table 3). These represent emblematic cases of catalyst self-adaptation and tuning, where the heterocomplexes perform better than the homocomplexes, and the conformationally mobile systems perform better than the rigid ones.

We are now actively investigating the use of combinations of *tropos* ligands for other enantioselective reactions.

Experimental Section

General procedure for the ligand library screening—Rh-catalyzed conjugate addition of arylboronic acid to enones: The reaction was performed using standard Schlenk techniques, under argon. A solution of the ligands (0.03 equiv, 0.006 mmol L^a + 0.03 equiv, 0.006 mmol L^b) and [{Rh(eth)$_2$Cl}$_2$] (0.015 equiv, 0.003 mmol, 5.8 mg) in degassed dioxane (0.5 mL) was stirred for 30 min. A solution of the appropriate arylboronic acid (2 equiv, 0.4 mmol) in degassed dioxane (0.3 mL) was added, followed by a 2 M KOH solution in water (1 equiv, 0.2 mmol, 0.1 mL). A solution of the substrate (1 equiv, 0.2 mmol) in dioxane (0.2 mL) was then added, and the reaction mixture was stirred overnight under argon, at the appropriate temperature. The reaction mixture was quenched with a saturated aqueous NaHCO$_3$ solution, and extracted with dichloromethane. The combined organic extracts were dried and concentrated in vacuo to give the crude product, which was purified by flash chromatography.

Acknowledgements

We thank the European Commission for financial support (R-Evolutionary Catalysis (REVCAT) MRTN-CT-2006–035866). We also thank Merck Research Laboratories (Merck's Academic Development Program

Award to C.G.) and Università degli Studi di Milano for financial support and for a postdoctoral fellowship to C.M. (Assegno di ricerca).

[1] For a recent review on the rhodium-catalyzed asymmetric conjugate addition, see: T. Hayashi, K. Yamasaki, *Chem. Rev.* **2003**, *103*, 2829–2844.

[2] a) Y. Takaya, M. Ogasawara, T. Hayashi, *J. Am. Chem. Soc.* **1998**, *120*, 5579–5580; b) Y. Takaya, T. Senda, H. Kurushima, M. Ogasawara, T. Hayashi, *Tetrahedron: Asymmetry* **1999**, *10*, 4047–4056; c) T. Hayashi, M. Takahashi, Y. Takaya, M. Ogasawara, *J. Am. Chem. Soc.* **2002**, *124*, 5052–5058; d) R. Amengual, V. Michelet, J. P. Genet, *Synlett* **2002**, 1791–1794.

[3] G. Chen, N. Tokunaga, T. Hayashi, *Org. Lett.* **2005**, *7*, 2285–2288.

[4] P. Mauleon, J. C. Carretero, *Org. Lett.* **2004**, *6*, 3195–3198.

[5] Q. Shi, L. Xu, X. Li, X. Jia, R. Wang, T. T.-L. Au-Yeung, A. S. C. Chan, T. Hayashi, R. Cao, *Tetrahedron Lett.* **2003**, *44*, 6505–6508.

[6] M. T. Reetz, D. Moulin, A. Gosberg, *Org. Lett.* **2001**, *3*, 4083–4085.

[7] M. Pucheault, S. Darses, J. P. Genet, *Eur. J. Org. Chem.* **2002**, 3552–3557.

[8] a) M. Kuriyama, K. Tomioka, *Tetrahedron Lett.* **2001**, *42*, 921–923; b) M. Kuriyama, K. Nagai, K. Yamada, Y. Miwa, T. Taga, K. Tomioka, *J. Am. Chem. Soc.* **2002**, *124*, 8932–8939; c) Y. Iguchi, R. Itooka, N. Miyaura, *Synlett* **2003**, 1040–1042; d) M. Kuriyama, T. Soeta, X. Hao, Q. Chen, K. Tomioka, *J. Am. Chem. Soc.* **2004**, *126*, 8128–8129.

[9] a) T. Hayashi, K. Ueyama, N. Tokunaga, K. Yoshida, *J. Am. Chem. Soc.* **2003**, *125*, 11508–11509; b) R. Shintani, K. Ueyama, I. Yamada, T. Hayashi, *Org. Lett.* **2004**, *6*, 3425–3427; c) Y. Otomaru, K. Okamoto, R. Shintani, T. Hayashi, *J. Org. Chem.* **2005**, *70*, 2503–2508; d) Y. Otomaru, A. Kina, R. Shintani, T. Hayashi, *Tetrahedron: Asymmetry* **2005**, *16*, 1673–1679; e) Y. Otomaru, N. Tokunaga, R. Shintani, T. Hayashi, *Org. Lett.* **2005**, *7*, 307–310; f) R. Shintani, K. Okamoto, T. Hayashi, *Org. Lett.* **2005**, *7*, 4757–4759; g) C. Defieber, J. Paquin, S. Serna, E. M. Carreira, *Org. Lett.* **2004**, *6*, 3873–3876; h) J. Paquin, C. R. J. Stephenson, C. Defieber, E. M. Carreira, *Org. Lett.* **2005**, *7*, 3821–3824.

[10] D. J. Weix, Y. Shi, J. A. Ellman, *J. Am. Chem. Soc.* **2005**, *127*, 1092–1093.

[11] R. T. Stemmler, C. Bolm, *J. Org. Chem.* **2005**, *70*, 9925–9931.

[12] a) J. G. Boiteau, F. Imbos, A. J. Minnaard, B. L. Feringa, *Org. Lett.* **2003**, *5*, 681–684 and 1385; b) A. Duursma, R. Hoen, J. Schuppan, R. Hulst, A. J. Minnaard, B. L. Feringa, *Org. Lett.* **2003**, *5*, 3111–3113; c) J. G. Boiteau, R. Imbos, A. J. Minnaard, B. L. Feringa, *J. Org. Chem.* **2003**, *68*, 9481–9484; d) Y. Iguchi, R. Itooka, N. Miyaura, *Synlett* **2003**, 1040–1042; e) A. Duursma, J. G. Boiteau, L. Lefort, J. A. F. Boogers, A. H. M. de Vries, J. G. de Vries, A. J. Minnaard, B. L. Feringa, *J. Org. Chem.* **2004**, *69*, 8045–8052; f) R. B. C. Jagt, J. G. de Vries, B. L. Feringa, A. J. Minnaard, *Org. Lett.* **2005**, *7*, 2433–2435; g) S. L. X. Martina, A. J. Minnaard, B. Hessen, B. L. Feringa, *Tetrahedron Lett.* **2005**, *46*, 7159–7163.

[13] For an account on *atropos*/*tropos* ligands, see: a) K. Mikami, K. Aikawa, Y. Yusa, J. J. Jodry, M. Yamanaka, *Synlett* **2002**, 1561–1578. For other recent work in this area, see also: b) K. Mikami, S. Kataoka, Y. Yusa, K. Aikawa, *Org. Lett.* **2004**, *6*, 3699–3701; c) P. Scafato, G. Cunsolo, S. Labano, C. Rosini, *Tetrahedron* **2004**, *60*, 8801–8806; d) X. Luo, Y. Hu, X. Hu, *Tetrahedron: Asymmetry* **2005**, *16*, 1227–1231; e) K. Mikami, K. Wakabayashi, K. Aikawa, *Org. Lett.* **2006**, *8*, 1517–1519; f) A. Iuliano, S. Facchetti, G. Uccello-Barretta, *J. Org. Chem.* **2006**, *71*, 4943–4950; g) K. Mikami, S. Kataoka, K. Wakabayashi, K. Aikawa, *Tetrahedron Lett.* **2006**, *47*, 6361–6364.

[14] a) C. Monti, C. Gennari, U. Piarulli, *Tetrahedron Lett.* **2004**, *45*, 6859–6862; b) C. Monti, C. Gennari, U. Piarulli, J. G. De Vries, A. H. M. De Vries, L. Lefort, *Chem. Eur. J.* **2005**, *11*, 6701–6717; c) C. Gennari, C. Monti, U. Piarulli, *Pure Appl. Chem.* **2006**, *78*, 303–310.

[15] For a preliminary communication on part of this work, see: C. Monti, C. Gennari, U. Piarulli, *Chem. Commun.* **2005**, 5281–5283.

[16] a) M. T. Reetz, T. Sell, A. Meiswinkel, G. Mehler, Patent Application DE-A 10247633.0, Oct. 11, **2002**; b) M. T. Reetz, T. Sell, A. Meiswinkel, G. Mehler, *Angew. Chem.* **2003**, *115*, 814–817; *Angew. Chem. Int. Ed.* **2003**, *42*, 790–793; c) M. T. Reetz, G. Mehler, *Tetrahedron Lett.* **2003**, *44*, 4593–4596; d) M. T. Reetz, G. Mehler, A. Meiswinkel, *Tetrahedron: Asymmetry* **2004**, *15*, 2165–2167; e) M. T. Reetz, X. Li, *Tetrahedron* **2004**, *60*, 9709–9714; f) M. T. Reetz, X. Li, *Angew. Chem.* **2005**, *117*, 3019–3021; *Angew. Chem. Int. Ed.* **2005**, *44*, 2959–2962; g) M. T. Reetz, X. Li, *Angew. Chem.* **2005**, *117*, 3022–3024; *Angew. Chem. Int. Ed.* **2005**, *44*, 2962–2964; h) M. T. Reetz, Y. Fu, A. Meiswinkel, *Angew. Chem.* **2006**, *118*, 1440–1443; *Angew. Chem. Int. Ed.* **2006**, *45*, 1412–1415.

[17] a) D. Peña, A. J. Minnaard, J. A. F. Boogers, A. H. M. de Vries, J. G. de Vries, B. L. Feringa, *Org. Biomol. Chem.* **2003**, *1*, 1087–1089; b) A. Duursma, D. Peña, A. J. Minnaard, B. L. Feringa, *Tetrahedron: Asymmetry* **2005**, *16*, 1901–1904; c) R. Hoen, J. A. F. Boogers, H. Bernsmann, A. J. Minnaard, A. Meetsma, T. D. Tiemersma-Wegman, A. H. M. de Vries, J. G. de Vries, B. L. Feringa, *Angew. Chem.* **2005**, *117*, 4281–4284; *Angew. Chem. Int. Ed.* **2005**, *44*, 4209–4212.

[18] For recent reviews on combinatorial ligand libraries and high-throughput experimentation in homogeneous catalysis, see: a) C. Gennari, U. Piarulli, *Chem. Rev.* **2003**, *103*, 3071–3100; b) J. G. de Vries, A. H. M. de Vries, *Eur. J. Org. Chem.* **2003**, 799–811; c) T. Satyanarayana, H. B. Kagan, *Adv. Synth. Catal.* **2005**, *347*, 737–748; d) J. G. De Vries, L. Lefort, *Chem. Eur. J.* **2006**, *12*, 4722–4734; e) C. Jäkel, R. Paciello, *Chem. Rev.* **2006**, *106*, 2912–2942.

[19] $[\{Rh(eth)_2Cl\}_2]$ is cheaper than the $[Rh(acac)(eth)_2]$ often used, and gave in this case comparable or better conversions and enantiomeric excesses.

[20] a) S. Sakuma, N. Miyaura, *J. Org. Chem.* **2001**, *66*, 8944–8946; b) R. Amengual, V. Michelet, J. P. Genet, *Tetrahedron Lett.* **2002**, *43*, 5905–5908; c) R. Itooka, Y. Iguchi, N. Miyaura, *J. Org. Chem.* **2003**, *68*, 6000–6004.

[21] F. Gini, B. Hessen, A. J. Minnaard, *Org. Lett.* **2005**, *7*, 5309–5312.

[22] F. Chen, A. Kina, T. Hayashi, *Org. Lett.* **2006**, *8*, 341–344.

[23] M. Oki, *Application of Dynamic NMR Spectroscopy to Organic Chemistry*, VCH, Weinheim, **1985**. See the Supporting Information for a detailed discussion and the relevant calculations.

[24] The energy barriers of model phosphites (containing either unsubstituted biphenol or 3,3′,5,5′-tetra-*tert*-butyl-2,2′-biphenol, and a P–OH bond) were calculated by semi-empirical MO methods (PM3) to be 4.4 and 7.5 kcal mol^{-1}, respectively; see: S. D. Pastor, S. P. Shum, R. K. Rodebaugh, A. P. Debellis, F. H. Clarke, *Helv. Chim. Acta* **1993**, *76*, 900–914. In the same paper, the free energy of activation for ring inversion of the dibenzo[*d*,*f*][1,3,2]dioxaphosphepine ring in a sterically congested biphenolic phosphite was determined by ^{31}P NMR spectroscopy and found to be 10.2–10.8 kcal mol^{-1}.

[25] a) A. Alexakis, S. Rosset, J. Allamand, S. March, F. Guillen, C. Benhaim, *Synlett* **2001**, 1375–1378; b) A. Alexakis, C. Benhaim, S. Rosset, M. Humam, *J. Am. Chem. Soc.* **2002**, *124*, 5262–5263; c) A. Alexakis, K. Croset, *Org. Lett.* **2002**, *4*, 4147–4149; d) A. Alexakis, D. Polet, C. Benhaim, S. Rosset, *Tetrahedron: Asymmetry* **2004**, *15*, 2199–2203; e) A. Alexakis, D. Polet, S. Rosset, S. March, *J. Org. Chem.* **2004**, *69*, 5660–5667; f) K. Tissot-Croset, D. Polet, A. Alexakis, *Angew. Chem.* **2004**, *116*, 2480–2482; *Angew. Chem. Int. Ed.* **2004**, *43*, 2426–2428; g) O. Equey, A. Alexakis, *Tetrahedron: Asymmetry* **2004**, *15*, 1531–1536; h) D. Polet, A. Alexakis, *Tetrahedron Lett.* **2005**, *46*, 1529–1532; i) K. Li, A. Alexakis, *Tetrahedron Lett.* **2005**, *46*, 5823–5826; j) K. Li, A. Alexakis, *Tetrahedron Lett.* **2005**, *46*, 8019–8022; k) M. d'Augustin, L. Palais, A. Alexakis, *Angew. Chem.* **2005**, *117*, 1400–1402; *Angew. Chem. Int. Ed.* **2005**, *44*, 1376–1378.

[26] For a variable-temperature ^{31}P NMR investigation of an iridium complex of a biphenolate ligand, see: A. Leitner, S. Shekhar, M. J. Pouy, J. F. Hartwig, *J. Am. Chem. Soc.* **2005**, *127*, 15506–15514.

[27] For the detection of two atropisomeric [Rh(Cl)(cod)P] species (in which P is a chiral biphenol-based phosphite) by ^{31}P NMR at

−65 °C, see: A. Suarez, A. Pizzano, I. Fernandez, N. Khiar, *Tetrahedron: Asymmetry* **2001**, *12*, 633–642.
[28] The chemical shift of this signal changed with the temperature, moving downfield as the temperature was lowered ($\delta = 157.3$, 159.6, and 161.3 ppm at 380, 300, and 230 K, respectively).
[29] Y. Cho, V. Zunic, H. Senboku, M. Olsen, M. Lautens, *J. Am. Chem. Soc.* **2006**, *128*, 6837–6846, and references therein.
[30] Similar monomer–dimer equilibria have been proposed recently; see reference [29].
[31] It has been observed that the $J_{P,Rh}$ value decreases on going from monomeric to dimeric complexes; see: a) H. L. M. Van Gaal, F. L. A. Van Den Bekerom, *J. Organomet. Chem.* **1977**, *134*, 237–248; b) G. E. Ball, W. R. Cullen, M. D. Fryzuk, W. J. Henderson, B. R. James, K. S. MacFarlane, *Inorg. Chem.* **1994**, *33*, 1464–1468; in our case, the doublet with coupling constant $J_{P,Rh} = 301$ Hz may be ascribed to the monomeric complex [L_2Rh(acac)] ($\delta = 160.3$ ppm) and the doublet with $J_{P,Rh} = 298$ Hz to the dimeric complex ($\delta =$ 159.2 ppm).
[32] B. Crociati, S. Antonaroli, M. L. Di Vona, S. Licoccia, *J. Organomet. Chem.* **2001**, *631*, 117–124.

Received: July 5, 2006
Published online: November 29, 2006

